

Fluorine Auger-electron production in collisions of H^+ and Li^{2+} with fluorocarbon targets

J. L. Shinpaugh, L. H. Toburen, and E. L. B. Justiniano

Department of Physics, East Carolina University, Greenville, North Carolina, 27858

(Received 22 June 1999)

Relative and absolute cross sections are presented for fluorine *KLL* Auger-electron production in collisions of 2.0-MeV H^+ and 0.5-MeV/amu Li^{2+} with various fluorocarbon targets. Auger yields were measured for molecular targets of CH_3F , CH_2F_2 , $C_2H_2F_2$, CHF_3 , CF_4 , C_2F_6 , and C_4F_8 . The fluorine Auger cross sections for these collision systems were found to be independent of the chemical environment, i.e., the atomic cross sections were found to obey additivity for these molecules. This is in contrast to recently reported fluorine *K*-shell ionization cross sections found for He^+ impact on fluorocarbon targets, where the atomic cross sections were found to differ by up to a factor of 3. [S1050-2947(99)50212-6]

PACS number(s): 34.50.Fa, 34.50.Gb, 32.80.Hd

The effect of the chemical environment on atomic collision processes, important for applications such as plasma chemistry and material processing, has been studied extensively over the past several decades. In fast ion-molecule collisions, collision processes have generally been described in terms of the additivity rule, where the total cross sections for the molecule are simply the sum of the cross sections of the constituent atoms (see, for example, Refs. [1–5]). In practice, additivity is used to determine atomic cross sections from molecular targets since few elements exist monoatomically.

Departures from additivity have been investigated for various collision processes in several ion-molecule collision systems. For charge transfer, corrections for multiple collisions of a projectile ion within a single molecule have been found to be important for determining electron-capture cross sections in collisions of protons with various hydrocarbons [6–8]. An intramolecular scattering model was developed to account for projectile-electron loss occurring subsequent to capture within the molecule. The corrections to the determined atomic cross sections were found to be as large as 25% in the regime where $\sigma_{capture} \ll \sigma_{loss}$.

Additivity failure has also been observed in atomic Auger-electron production cross sections from molecular targets [1,9,10]. Again, intramolecular multiple scattering was found to play an important role. In this case, inelastic scattering of the Auger electron by the constituent atoms of the molecule accounted for up to a 30% difference in the yields per atom between various molecular targets. Consequently, accurate determination of *K*-shell ionization cross sections from Auger-electron yields required including multiple-scattering effects.

While chemical effects have been found to affect atomic cross sections in ion-molecule collisions significantly, in general these effects have been observed to exist in the range of approximately 30% or less. In contrast, recent measurements of cross sections using fluorocarbon targets showed dramatic departures from additivity, where fluorine *K*-shell ionization cross sections were reported to differ by as much as a factor of 3 for He^+ bombardment of $C_2H_2F_2$, C_2F_6 , and C_4F_8 [11]. To explore this effect further, we have measured relative and absolute cross sections for *KLL* Auger-electron

production for collisions of 2.0-MeV protons and 0.5 MeV/amu Li^{2+} ions incident on various fluorocarbon targets.

The measurements were performed using the 2-MV tandem Van de Graaff accelerator at East Carolina University (ECU). For each experiment, negative H or Li ions were extracted from a cesium-sputter ion source and injected into the accelerator. The H^+ or Li^{2+} ion beam from the accelerator was momentum analyzed, collimated, and directed into a scattering chamber. Doubly differential cross sections for electron emission were measured using an analysis system on loan to ECU from Pacific Northwest National Laboratory. This system has been described in detail previously [12], having been used by Toburen, DuBois, and co-workers for over 20 years. Briefly, this system consists of a magnetically shielded chamber with external Helmholtz coils for minimizing the magnetic field in the chamber. The ion beam, highly collimated by entrance apertures into the chamber, passed through a target-gas interaction region and was collected in a Faraday cup. The target gas was injected into the interaction region through a collimated-holes structure with a 100:1 length-to-diameter ratio. The gas inlet pressure behind the collimated-holes structure was held constant using a capacitance-manometer-controlled automatic leak valve. Typical inlet pressures of 100 to 200 μ m were chosen to insure single-collision conditions for the target density in the interaction region. At these inlet pressures, the collision-chamber pressure was $\leq 10^{-5}$ Torr.

Electrons emitted in collisions of the ion beam with the target were electrostatically analyzed using a cylindrical-mirror analyzer and detected by a channel electron multiplier. Electron-energy spectra were acquired by stepping the analyzer voltage, and thus the electron pass energy, with the integrated beam current. The analyzer was rotated about the interaction region and spectra were recorded from 10° to 140° with respect to the incident beam direction in 5° and 10° intervals. The energy and angular resolution of the analyzer was approximately 3.5% and 2° , respectively. Electron yields as a function of electron energy and emission angle were measured for collisions of 2.0-MeV H^+ and 3.5-MeV Li^{2+} ions incident on fluorocarbon targets of CH_3F , CH_2F_2 , $C_2H_2F_2$, CHF_3 , CF_4 , C_2F_6 , and C_4F_8 for electron energies up to 800 eV, well above the F Auger peak.

Relative doubly differential cross sections at a given target pressure were determined from the electron yields. Normalization for the target density was accomplished by integrating the doubly differential cross sections over emission angle and comparing the resulting singly differential cross sections to the Rutherford energy-loss cross section. This method is based upon the premise that the continuum electron yields in collisions of fast protons with atoms and molecules are accurately predicted by the Rutherford energy-loss cross section at sufficiently high electron energies [13–17]. Using this technique, the effective target density is determined directly from the continuum electron yield, and does not rely on assumptions of the dynamic target pressure in the beam-target interaction region.

In this method, relative doubly differential cross sections at a given target-gas pressure were determined from the electron yields and the integrated beam current, correcting for the electron-energy dependence of the channeltron detection efficiency and for the dependence of the solid angle and effective target thickness on the emission angle:

$$\sigma_{rel}(\epsilon, \theta) = \frac{N_e}{N_p \epsilon d_{eff}(\epsilon) \Omega l(\theta)},$$

where N_e and N_p are the number of detected electrons and incident protons, respectively, and ϵ is the electron energy. The correction for solid angle and effective target length, $\Omega l(\theta)$, was determined by measuring the K -Auger yields from neon, oxygen, and nitrogen targets, assuming isotropic emission. The channeltron detection efficiency $d_{eff}(\epsilon)$ was taken from previous measurements of the efficiency [18], which was found to be unity for electron energies up to 600 eV, then decreased linearly to 78% at 2200 eV. It may be noted that the final cross-section values are relatively insensitive to the value of the efficiency. Integrating the relative doubly differential cross sections over the emission angle gives the relative singly differential cross sections,

$$\sigma_{rel}(\epsilon) = 2\pi \int_0^\pi \sigma_{rel}(\epsilon, \theta) \sin\theta d\theta.$$

The singly differential cross sections were then normalized to the Rutherford energy-loss cross section, scaled for the number of electrons in the target molecule. The Rutherford cross section (per electron) is given by

$$\frac{d\sigma_R}{dE} = \frac{4\pi a_0^2 Z^2 R^2}{T E^2},$$

where a_0 is the Bohr radius, Z is the projectile charge, R is the Rydberg energy, T is the reduced projectile energy, and E is the energy transferred to the electron [19]. The reduced projectile energy is equal to $\frac{1}{2} m v^2$, where m is the electron mass and v is the incident projectile velocity. For our purposes, we have taken the energy loss as the electron energy minus the first ionization potential of the target, $E = \epsilon - I$. Since the Rutherford cross section is defined per electron, the ratio of the measured singly differential cross sections to the

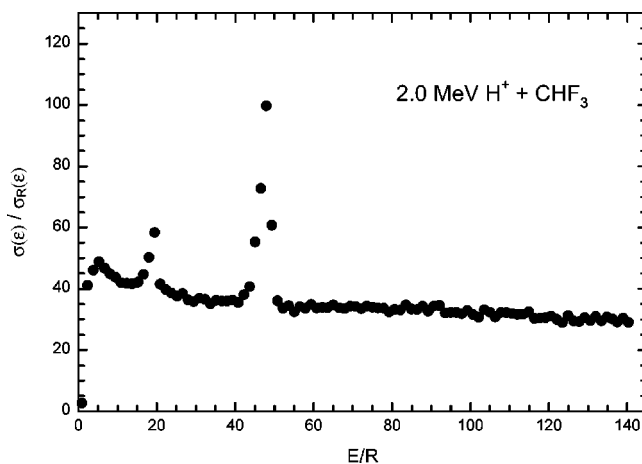


FIG. 1. The ratio of the measured singly differential cross section to the Rutherford energy-loss cross section plotted as a function of the energy loss for a 2.0-MeV proton incident on CHF_3 .

Rutherford cross section should be a constant, equal to the number of electrons in the target molecule (where the Rutherford cross section is valid, at high electron energies). This ratio is shown in Fig. 1 as a function of energy loss for CHF_3 . It can be seen that for E/R values greater than approximately 60 (corresponding to $\epsilon \geq 800$ eV), the ratio is constant. This gives then the absolute normalization for both the singly and doubly differential cross sections.

The fluorine KLL Auger cross sections for the various fluorocarbon targets were determined from the absolute doubly differential cross sections taken in high resolution at 110° emission angle. A typical spectrum, along with the fit to the continuum electron yield in the region above and below the F Auger peak, is shown in Fig. 2 for 2-MeV protons incident on C_4F_8 . The total cross section per molecule was found by subtracting the continuum electron intensity in the region of the peak, integrating over energy, and multiplying by 4π steradians (assuming isotropic emission). Dividing by the number of fluorine atoms in the molecule then gives the total cross section per atom. Table I lists the cross sections for fluorine KLL Auger-electron production per F atom found for the various fluorocarbon targets.

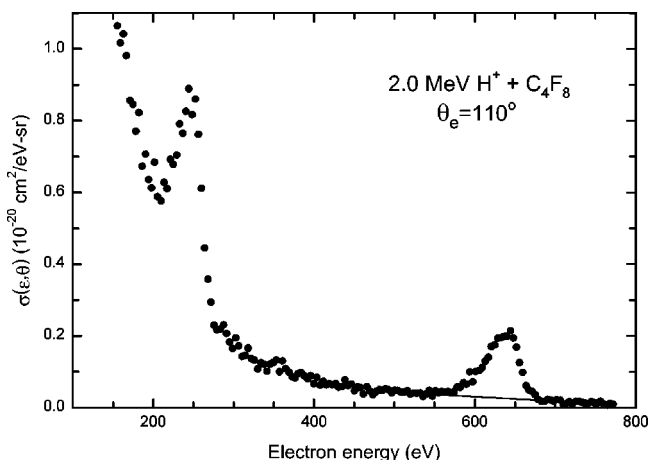


FIG. 2. Doubly differential cross section for electron emission in collisions of 2.0-MeV H^+ with C_4F_8 . The solid line is the fit to the continuum-electron yield in the region of the F Auger peak.

TABLE I. Cross sections for F Auger-electron production in collision of 2-MeV H^+ and 3.5-MeV Li^{2+} with fluorocarbon targets in units of 10^{-19} cm^2 . Error bars given are for relative uncertainties only. Absolute errors are 30%.

Target	σ	
	2-MeV H^+	3.5-MeV Li^{2+}
CH_3F	1.31 ± 0.16	6.99 ± 0.98
CH_2F_2	1.56 ± 0.19	6.78 ± 0.95
$C_2H_2F_2$	1.47 ± 0.18	7.10 ± 0.99
CHF_3	1.36 ± 0.16	6.66 ± 0.93
CF_4	1.58 ± 0.19	6.50 ± 0.91
C_2F_6	1.65 ± 0.20	8.13 ± 1.14
C_4F_8	1.50 ± 0.18	7.36 ± 0.88

Since the fluorescence yields for second-row elements are less than 1%, direct comparison can be made between the Auger yields and K -shell ionization cross sections. The general trend found by Ghebremedhin *et al.* [11] showed a decreasing K -shell ionization cross section with the increasing number of fluorine atoms in the target molecule for He^+ impact on $C_2H_2F_2$, C_2F_6 , and C_4F_8 . For 0.5-MeV/amu He^+ impact, the cross section *per fluorine atom* differed by more than a factor of 2 for C_4F_8 and $C_2H_2F_2$. Included in these results were corrections for intramolecular secondary scattering of the Auger electron. This effect was calculated to be a 5–10% correction to the cross sections, and did not account for the large variation between molecules. For the equal-velocity system reported here, 0.5-MeV/amu Li^{2+} , the measured cross sections for fluorine K -Auger yields do not show a statistically significant dependence on the molecular target involved in the collision.

Presumably, secondary scattering of the Auger electron from Li^{2+} impact should be similar to that for He^+ impact. Even so, since Li^{2+} ions are more perturbing to the target than He^+ , possible differences in the measured electron yields conceivably could arise from the interaction of the various molecules with the two different projectile ions. Greater fragmentation of the larger molecules by Li^{2+} could produce a different molecular dependence in the cross sec-

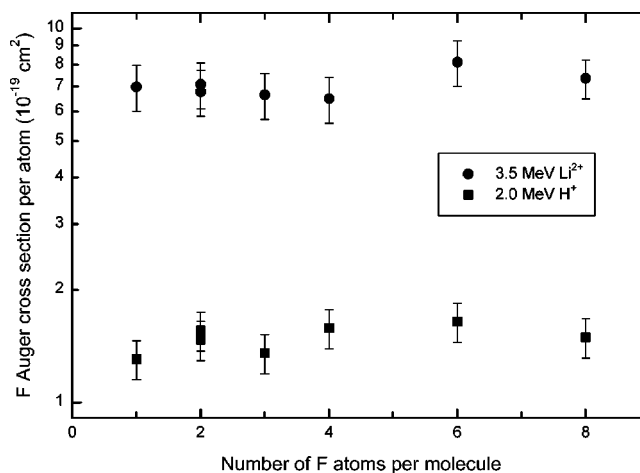


FIG. 3. Cross sections for F Auger-electron production in collisions of 2-MeV H^+ and 3.5-MeV Li^{2+} with CH_3F , CH_2F_2 , $C_2H_2F_2$, CHF_3 , CF_4 , C_2F_6 , and C_4F_8 , plotted as a function of the number of fluorine atoms in the target molecule. Error bars shown are for relative uncertainties only. Absolute errors are 30%.

tions than He^+ . To investigate this possibility, 2.0-MeV protons were chosen to produce inner-shell ionization that would provide the least perturbation on the molecule (sometimes referred to as needle ionization). These results, as seen in Table I, also do not show a significant dependence on the molecular environment of the target. The observed target dependences for both collision systems of the present work are illustrated in Fig. 3, where the cross sections are presented as a function of the number of fluorine atoms in the target molecule.

In conclusion, we have presented the cross sections for fluorine KLL Auger-electron production measured for collisions of 2.0-MeV H^+ and 0.5-MeV/amu Li^{2+} with various fluorocarbon targets. The Auger yields per fluorine atom were found to be independent of the molecular environment of the fluorine for these collision systems. These results are in contrast to recently reported cross sections for He^+ impact on fluorocarbon targets.

This work was supported in part by the Research Corporation.

- [1] L. H. Toburen, *Phys. Rev. A* **5**, 2482 (1972).
- [2] N. Stolterfoht, in *Proceedings of the International Conference on Inner Shell Ionization Phenomena and Future Applications*, edited by R. W. Fink, S. T. Manson, J. M. Palms, and P. Vanugopala, CONF-720404 (USAEC, Oak Ridge, TN, 1973), p. 979.
- [3] R. P. Chaturvedi, D. J. Lynch, L. H. Toburen, and W. E. Wilson, *Phys. Lett.* **61A**, 3674 (1977).
- [4] G. Bissinger, J. M. Joyce, J. A. Tanis, and S. L. Varghese, *Phys. Rev. Lett.* **44**, 241 (1980).
- [5] T. R. Dillingham, B. M. Doughty, J. M. Hall, T. N. Tipping, J. M. Sanders, and J. L. Shinpaugh, *Nucl. Instrum. Methods Phys. Res. B* **40/41**, 40 (1989).
- [6] G. Bissinger, J. M. Joyce, G. Lapicki, R. Laubert, and S. L. Varghese, *Phys. Rev. Lett.* **49**, 318 (1982).
- [7] S. L. Varghese, G. Bissinger, J. M. Joyce, and R. Laubert, *Phys. Rev. A* **31**, 2202 (1985).
- [8] G. Bissinger, *Nucl. Instrum. Methods Phys. Res. B* **99**, 210 (1995).
- [9] D. L. Mathews and F. Hopkins, *Phys. Rev. Lett.* **40**, 1326 (1978).
- [10] R. D. McElroy, Jr., W. M. Ariyasinghe, and D. Powers, *Phys. Rev. A* **36**, 3674 (1987).
- [11] A. Ghebremedhin, W. M. Ariyasinghe, and D. Powers, *Phys. Rev. A* **53**, 1537 (1996).
- [12] L. H. Toburen, R. D. DuBois, C. O. Reinhold, D. R. Schultz, and R. E. Olson, *Phys. Rev. A* **42**, 5338 (1990).
- [13] Y.-K. Kim, *Radiat. Res.* **61**, 21 (1975).
- [14] L. H. Toburen, W. E. Wilson, and L. E. Porter, *J. Chem. Phys.* **67**, 4212 (1977).

- [15] L. H. Toburen, S. T. Manson, and Y.-K. Kim, *Phys. Rev. A* **17**, 148 (1978).
- [16] L. H. Toburen, in *Physical and Chemical Mechanisms in Molecular Radiation Biology*, edited by W. A. Glass and M. N. Varma (Plenum Press, New York, 1991), p. 51.
- [17] N. Stolterfoht, R.D. DuBois, and R.D. Rivarola, *Electron Emission in Heavy Ion-Atom Collisions* (Springer, New York, 1997), Chap. 3, Sec. 1.
- [18] L. H. Toburen, *Phys. Rev. A* **3**, 216 (1971).
- [19] M. E. Rudd, Y.-K. Kim, D. H. Madison, and T. J. Gay, *Rev. Mod. Phys.* **64**, 441 (1992).